Cancer Cell
Article

The Extracellular Matrix Protein TGFBI Induces Microtubule Stabilization and Sensitizes Ovarian Cancers to Paclitaxel

Ahmed Ashour Ahmed,[1,3,5] Anthony D. Mills,[4] Ashraf E.K. Ibrahim,[1] Jillian Temple,[1,3] Cherie Blenkiron,[3] Maria Vias,[3] Charlie E. Massie,[3] N. Gopalakrishna Iyer,[3] Adam McGeoch,[4] Robin Crawford,[5] Barbara Nicke,[6] Julian Downward,[6] Charles Swanton,[6] Stephen D. Bell,[4] Helena M. Earl,[3] Ronald A. Laskey,[4] Carlos Caldas,[2,3] and James D. Brenton[1,3,*]

[1]Functional Genomics of Drug Resistance Laboratory
[2]Breast Cancer Functional Genomics Laboratory
Cancer Research UK Cambridge Research Institute, Li Ka Shing Centre, Robinson Way, Cambridge CB2 0RE, UK
[3]Department of Oncology
[4]MRC Cancer Cell Unit
Hutchison/MRC Research Centre, Hills Road, Cambridge, CB2 0XZ, UK
[5]Gynaecological Oncology Regional Centre, Box 242, Addenbrooke's Hospital, Cambridge University Hospitals NHS Foundation Trust, Hills Road, Cambridge CB2 0QQ, UK
[6]Signal Transduction Laboratory, Cancer Research UK London Research Institute, 44 Lincoln's Inn Fields, London WC2A 3PX, UK
*Correspondence: james.brenton@cancer.org.uk
DOI 10.1016/j.ccr.2007.11.014

SUMMARY

The extracellular matrix (ECM) can induce chemotherapy resistance via AKT-mediated inhibition of apoptosis. Here, we show that loss of the ECM protein TGFBI (transforming growth factor beta induced) is sufficient to induce specific resistance to paclitaxel and mitotic spindle abnormalities in ovarian cancer cells. Paclitaxel-resistant cells treated with recombinant TGFBI protein show integrin-dependent restoration of paclitaxel sensitivity via FAK- and Rho-dependent stabilization of microtubules. Immunohistochemical staining for TGFBI in paclitaxel-treated ovarian cancers from a prospective clinical trial showed that morphological changes of paclitaxel-induced cytotoxicity were restricted to areas of strong expression of TGFBI. These data show that ECM can mediate taxane sensitivity by modulating microtubule stability.

INTRODUCTION

Taxanes are microtubule-stabilizing drugs that have been extensively used as effective chemotherapeutic agents in the treatment of solid tumors (McGuire et al., 1996; Sandler et al., 2006). However, taxane resistance limits clinical utility to approximately 50% of patients with breast or ovarian cancer. Identification of mechanisms of taxane resistance that are therapeutically accessible is, therefore, required to improve treatment.

Paclitaxel, a prototype taxane, stabilizes microtubule polymers leading to mitotic arrest and apoptosis (Schiff et al., 1979; Ibrado et al., 1998; Scatena et al., 1998). General mechanisms of drug resistance, including overexpression of the ABC/MDR transporter family of proteins (Peer et al., 2004), delayed G2/M transition (Tan et al.,

SIGNIFICANCE

Extracellular matrix (ECM) proteins such as fibronectin induce resistance to chemotherapy via activation of intracellular survival pathways. We now show that the ECM protein TGFBI mediates specific sensitization to paclitaxel by inducing stabilization of microtubules via integrin-mediated signaling pathways. Analysis of paclitaxel-treated ovarian cancers from a prospective clinical trial shows TGFBI protein expression in areas of paclitaxel-induced cytotoxicity. Bioinformatic analysis of three microarray expression data sets from 223 ovarian and breast cancer samples show that *TGFBI* expression is tightly coregulated with other genes that induce paclitaxel sensitization such as *THBS1*. These data show that paclitaxel response can be modulated by ECM proteins and raise the prospect of improving the therapeutic index of taxanes via manipulation of these proteins and their downstream signaling pathways.

2002), defective mitotic checkpoints (Anand et al., 2003), and alterations in apoptosis regulation (Huang et al., 1997), may alter paclitaxel sensitivity. More specifically, alterations of microtubules induce severe taxane resistance (Zhang et al., 1998; Gonçalves et al., 2001; Alli et al., 2002; Wang et al., 2004). These include β-tubulin mutations which may decrease paclitaxel binding to microtubules (Giannakakou et al., 1997). Alternatively, factors that increase the ratio of unstable to stable microtubules induce profound taxane resistance. This may occur by mutations in nonpaclitaxel binding sites, alterations in tubulin isoforms (Gonçalves et al., 2001; Barlow et al., 2002; Hari et al., 2006), overexpression of β-III tubulin (Mozzetti et al., 2005), and overexpression of the microtubule-associated protein stathmin (Alli et al., 2002).

Cells contain subsets of stable and dynamic microtubules that are functionally distinct (Gundersen et al., 1984), and there is strong evidence that extracellular stimuli regulate microtubule stability. Serum starvation or loss of direct cell contact results in loss of microtubule stabilization, while fibronectin-mediated adhesion or treatment of cells with lysophosphatidic acid or TGFβ induce microtubule stability (Cook et al., 1998; Palazzo et al., 2004; Gundersen et al., 1994). Whether extracellular matrix (ECM) modulation of microtubule stability may alter paclitaxel sensitivity has been, to date, unknown.

We describe here the identification of TGFBI (transforming growth factor beta induced) as an ECM protein that induces microtubule stabilization and modulates paclitaxel sensitivity in vitro and in patients receiving paclitaxel therapy.

RESULTS

TGFBI Is Significantly Underexpressed in an Ovarian Cancer Cell Line Model of Paclitaxel Resistance

To identify genes associated with the acquisition of paclitaxel resistance, we studied the ovarian cancer cell line SKOV-3TR, which was derived from SKOV-3 by prolonged and repeated exposure to increasing doses of paclitaxel (Duan et al., 1999). We compared the expression profiles of the parent and resistant lines using cDNA microarrays (Figure 1A) after confirming that SKOV-3 and SKOV-3TR were isogenic by short tandem repeats genotyping (data not shown). Examination of the most differentially expressed genes showed several candidates previously identified in chemotherapy response including *CP*, *SOD2* (Ueta et al., 2001), *HMGA1* (Huang et al., 1994; Kasparkova et al., 2003), and *CXCL1* (Taxman et al., 2003) (Figure 1A; Table S1 in the Supplemental Data available with this article online).

The most underexpressed gene in the taxane-resistant line was transforming growth factor beta induced (*TGFBI*; also known as Big-h3, β-ig H3, and keratoepithelin), which is an extracellular matrix protein whose secretion is induced by TGFβ1 stimulation (Skonier et al., 1992). Its functions include cell adhesion to the ECM and integrin-mediated signaling (Jeong and Kim, 2004; Billings et al., 2002). Quantitative real-time PCR confirmed striking underexpression (>1000 fold) of *TGFBI* (Figure 1B). This underexpression was maintained after growing the cells without paclitaxel for several months (data not shown). Immunocytochemistry using anti-TGFBI antibody on paraffin-embedded cell blocks and immunoblotting of conditioned media from the two cell lines showed very low secretion of TGFBI protein (Figures 1C and 1D) from the resistant SKOV-3TR cells.

Loss of *TGFBI* Is Sufficient to Induce Paclitaxel Resistance

To examine the effect of loss of *TGFBI* expression on paclitaxel sensitivity, stable transfected cell lines expressing short interfering RNAs (siRNA) against *TGFBI* were generated from the parental SKOV-3 line. Two vectors targeting 21 bp sequences at nucleotides 810 or 1318 of the *TGFBI* coding sequence were transfected independently or together to generate stable cell line pools SKOV3-A, SKOV3-K, and SKOV3-AK, respectively. Effective knockdown (KD) of *TGFBI* mRNA and protein was achieved in all three lines (Figures 1B and 1D and data not shown).

The effect of paclitaxel treatment on these cells was examined. Early apoptosis was measured after 48 hr of paclitaxel exposure by flow cytometry of cells stained with FITC-annexin V and 7-AAD (Wang et al., 1998). Cell lines that lacked *TGFBI* (SKOV-3TR and *TGFBI*-KD cells) showed a significantly lower percentage of paclitaxel-induced apoptosis ($p < 0.001$, one-way ANOVA) in contrast to control SKOV-3 cells (Figure 1E). Caspase 3/7 activation 48 hr following paclitaxel treatment was significantly reduced in SKOV-3TR and *TGFBI*-KD cells ($p < 0.001$, two-way ANOVA) (Figure 1F) as was caspase 3 cleavage (Figure S1A).

Analysis of 9 ovarian and 11 breast cancer cell lines showed that *TGFBI* expression was significantly lower in resistant ($n = 7$) cells ($p = 0.027$, two-way ANOVA), and this was independent of cell type (Figures S1B and S1C). Importantly, transient knockdown of *TGFBI* using a pool of four siRNAs in four additional ovarian cancer cell lines, OVCAR3 (Figure 1G), TR175 (Figure 1H), 1847 (Figure S1D), and PE01 (Figure S1E), resulted in significant resistance to paclitaxel-induced caspase activation ($p < 0.001$, two-way ANOVA). These results were confirmed using at least two individual siRNAs in each cell line (data not shown).

SKOV-3TR cells have accumulated multiple paclitaxel resistance mechanisms during in vitro selection (Lamendola et al., 2003). For example, expression profiling of SKOV-3TR shows upregulation of *MDR1* and *ABCB6* (Duan et al., 2005; data not shown). The intensity values of a fluorescent derivative of paclitaxel were lower in SKOV-3TR compared to parental SKOV-3 and could be corrected using the MDR1 inhibitor verapamil (Figure S2A). However, induction of paclitaxel resistance in SKOV-3 cells by specific downregulation of *TGFBI* strongly suggested that *TGFBI* was an important component of the resistance shown in SKOV-3TR.

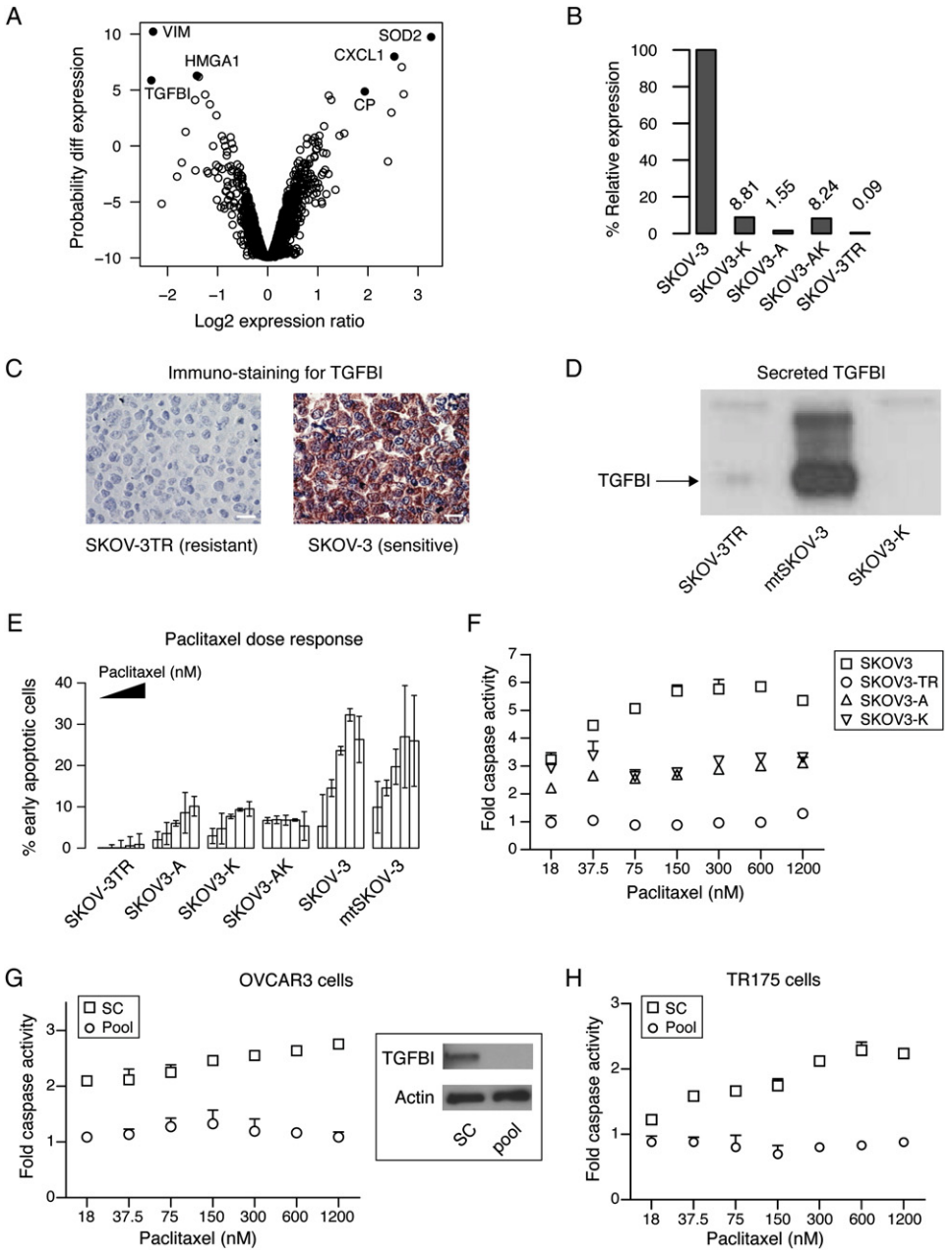

Figure 1. Loss of *TGFBI* Is Sufficient to Induce Paclitaxel Resistance

(A) Volcano plot shows log fold change in gene expression in the paclitaxel-resistant cell line SKOV-3TR compared to the sensitive parental line SKOV-3 and plotted against the likelihood of differential expression. Note that negative log2 expression ratios indicate underexpression in SKOV-3TR. Data points represent the probability value for differential gene expression and data shown is from four replicate experiments.

(B) Relative expression levels of *TGFBI* in different cell lines using real time PCR.

(C) Immunocytochemistry of stained sections from embedded cell pellets using anti-TGFBI antibody. Scale bars, 10 μm.

(D) Western blotting of culture medium from SKOV-3TR, mock-transfected SKOV-3, and *TGFBI* siRNA-transfected SKOV3-K cell lines probed with anti-TGFBI antibody.

(E) Effect of stable KD of *TGFBI* (SKOV3-A, SKOV3-K, and SKOV3-AK) on paclitaxel-induced apoptosis measured by FITC-annexin V and 7-AAD staining at 48 hr following paclitaxel treatment (150, 300, 600, 1200, and 2000 nM) compared to SKOV-3, mock-transfected SKOV-3 (mtSKOV3), and SKOV-3TR cells. Filled triangle indicates increasing paclitaxel dose across each group of bars.

(F) Effect of stable KD of *TGFBI* on caspase 3/7 activation 48 hr following paclitaxel treatment.

(G and H) Transient *TGFBI*-KD in OVCAR3 and TR175 lines induces paclitaxel resistance. Caspase 3/7 activation was estimated 48 hr following transfection using either a pool of 4 siRNAs targeting *TGFBI* or nontargeting scrambled controls (sc). OVCAR3 cells (G) or TR175 cells (H) were treated with paclitaxel for 48 hr. Immunoblot confirming knockdown of TGFBI protein is shown in (G). Error bars show mean ± SD.

To investigate how *TGFBI* modulated response to paclitaxel, we analyzed common resistance mechanisms using *TGFBI*-KD cells. Intracellular intensity of fluorescent paclitaxel was not different after *TGFBI*-KD (Figure S2A). In addition, apoptosis induction using UV, cisplatin, or nocodazole treatment was not significantly different between *TGFBI*-KD and parental cells (Figure S2B). These data show that paclitaxel resistance arising from specific loss of *TGFBI* is not caused by nonspecific alterations in apoptotic or multi-drug-resistance pathways.

Abnormal mitotic checkpoints have previously been shown to confer paclitaxel resistance (Anand et al., 2003). Mitotic SKOV-3 cells lacking *TGFBI* showed a slight increase in prophase (Figure S2C), but no significant difference in the duration of mitotic progression was observed when measured by time-lapse imaging of individual cells ($p = 0.1$, one-way ANOVA, Figure S2D). A characteristic feature of overriding mitotic checkpoints is persistence of checkpoint proteins following metaphase (Anand et al., 2003). Figure S2E shows no significant difference ($p = 0.4$, Chi Square test) between KD and control cell lines in the proportion of postmetaphase cells showing persistent cyclin B1 staining. BubR1, a mitotic checkpoint protein expressed prior to anaphase, is thought to sense tension across the spindle when chromosomes are aligned in the metaphase plate (Nicklas, 1997). Correct sensing of spindle tension leads to degradation of BubR1 and anaphase transition. Spindle poisons such as nocodazole and paclitaxel abolish tension leading to persistent expression of BubR1 (Logarinho et al., 2004). Cells with abnormal BubR1 function progress to anaphase in spite of exposure to spindle poisons. The expression of BubR1 in wild-type, KD, and SKOV-3TR cells was normal following nocodazole treatment indicating that sensing of spindle tension was not impaired (Figure S2F). Delayed cell-cycle transition has been shown to confer paclitaxel resistance (Tan et al., 2002). There was no difference in cell-cycle profiles of nonsynchronized *TGFBI*-KD or SKOV-3TR cells as compared to mock-transfected SKOV-3 (data not shown). To test cell-cycle profiles in synchronized cells, we used HeLa cells as they express comparable levels of TGFBI to those of SKOV-3 (data not shown) and are a well characterized cell-cycle model with intact mitotic checkpoints and are sensitive to paclitaxel (Anand et al., 2003). Figure S2G shows that transient knockdown of *TGFBI* had no effect on cell-cycle progression in HeLa cells synchronized in G1 by double thymidine block.

TGFBI Restores Paclitaxel-Induced Tubulin Polymerization

Microtubule bundle formation has been described as the hallmark of paclitaxel exposure in vivo (Schiff and Horwitz, 1980) and is lost in resistant cells (Giannakakou et al., 1997). Indeed, SKOV-3 cells treated with 2 μM paclitaxel for 24 hr showed striking paclitaxel-induced bundles (PIBs) in interphase cells (Figures 2A and 2B and Figure S3A) and severe failure of mitotic spindle organization. Mitotic cells showed a prometaphase-like state where chromosomes formed ring-like structures around centrally radiating microtubule fibers, which we termed mitosis-like wheels (MLWs) (Figure S3B). In contrast, a minority of SKOV-3TR cells showed PIBs (2.4% versus 93%) or MLWs (1.7% versus 92%) (Figures 2C and 2D and Figure S3A). Importantly, SKOV-3TR cells transfected with a myc-tagged *TGFBI* expression plasmid (pCSMT-*TGFBI*) showed a modest increase (12% versus 3.7%) in the proportion of PIBs and MLWs following paclitaxel treatment ($p < 0.001$, two-sided t test) (Figures 2E and 2F and Figure S3A).

Paclitaxel induces microtubule stabilization, and post-translational modifications of tubulin, such as detyrosination or acetylation, accumulate in these stable microtubules. Detyrosination exposes Glu residues at the carboxy terminus of alpha-tubulin that can be detected using antibodies and, therefore, used as a marker of microtubule stability (Gundersen et al., 1984). Cells lacking *TGFBI* (SKOV-3TR, SKOV3-K) showed impaired paclitaxel-induced microtubule stabilization as evidenced by decreased Glu-tubulin formation following paclitaxel treatment (Figure 2G). Similarly, transient *TGFBI*-KD of SKOV-3 using pooled siRNAs resulted in intermediate reduction of paclitaxel induced Glu-tubulin (Figure 2G). These data suggest that selective loss of *TGFBI* induces paclitaxel resistance at the level of microtubules. Alteration of microtubule function leading to paclitaxel resistance is associated with increased ratios of soluble to insoluble intracellular tubulin (Gonçalves et al., 2001; Barlow et al., 2002; Hari et al., 2006). Consistent with this, SKOV-3TR and SKOV3-K cells showed increased soluble tubulin compared to parental SKOV-3 cells (Figures 2H and 2I).

TGFBI Silencing Results in Increased Mitotic Abnormalities in Cancer Cell Lines

Tight regulation of tubulin dynamics is crucial for normal completion of mitosis, and alterations in microtubules that induce taxane resistance can cause geometric deformities in the mitotic spindle (Gonçalves et al., 2001; Kline-Smith and Walczak, 2004). Mitotic cells from SKOV-3TR had a significantly higher proportion of abnormal mitosis compared to control SKOV-3 cells (14% versus 1.9%, respectively; $p < 0.001$, two-way ANOVA) (Figure 3C). To confirm that loss of *TGFBI* was sufficient to induce mitotic abnormalities, we examined the effects of *TGFBI* knockdown on mitosis in SKOV3-K and SKOV3-A cells. Strikingly, abnormal mitotic figures were observed including monopolar spindle formation, multiple centrosomes with multipolar spindles (Figure 3A), and abnormal spindle architecture (Figure 3B) in stably transfected cells 9–30 days following transfection. Control cells transfected with empty vector and examined in parallel at the same time points did not show significant mitotic abnormalities (Figure 3C). In addition, interphase cells showed a significant increase in the proportion of cells with centrosome amplification (Figure 3D). These phenotypes were also observed 48 hr after transient *TGFBI*-KD of HeLa, 1847, and OVCAR3 cell lines and also in SKOV-3 using A810 and

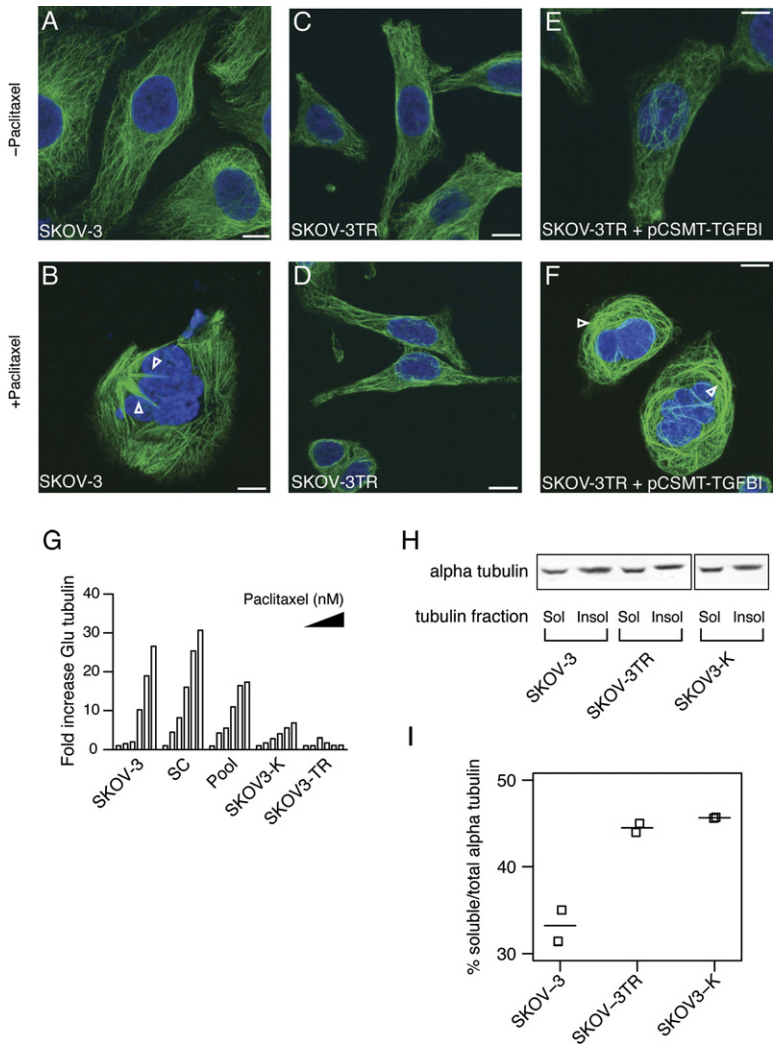

Figure 2. Loss of *TGFBI* Causes Defective Paclitaxel-Induced Microtubule Polymerization

(A–F) Overexpression of *TGFBI* in SKOV-3TR by pCSMT-*TGFBI* sensitizes microtubules to the polymerizing effect of paclitaxel. Arrowheads indicate paclitaxel-induced bundles (PIBs). Green, tubulin; blue, Dapi-stained DNA. Scale bars, 10 μm.

(G) Paclitaxel induces Glu-tubulin formation. Cells were serum starved for 24 hr then treated with paclitaxel in serum-free medium (SFM) at 0, 4, 16, 75, 300, and 1200 nM concentrations for 1 hr. Lysates were collected for fluorescence immuno-blotting with anti-Glu-tubulin and anti-alpha tubulin. Bars represent the fold increase in Glu-tubulin fluorescence intensity values normalized for alpha-tubulin intensity values. Filled triangle indicates increasing paclitaxel dose across each group of bars.

(H) A fluorescence immunoblot of soluble (sol) and insoluble (insol) tubulin fractions.

(I) SKOV-3TR and SKOV3-K cells have increased soluble tubulin. Graph shows the percentages of soluble tubulin in relation to total tubulin in the different cell lines. Quantitative measurements were performed using fluorescence immunoblotting with anti-alpha tubulin antibody as described in Supplemental Experimental Procedures. Results shown are from two independent experiments. Horizontal bars indicate median values.

K1318 constructs, although lower proportions of abnormal mitoses were seen (Figure 3E and data not shown).

To examine whether direct colocalization of TGFBI with microtubules or centrosomes could explain these findings, we characterized the subcellular localization of carboxy-terminal tagged TGFBI (with green fluorescent protein or myc epitopes). Tagged-TGFBI localized in the Golgi apparatus and in intracellular vesicles along microtubule fibers and accumulated at cellular protrusions consistent with secretion (Figure S4). No tagged-TGFBI was seen in the nucleus of interphase cells and there was no localization in mitosis to spindle poles, spindle fibers, or condensed chromosomes.

rTGFBI Protein Promotes Cell Adhesion and Microtubule Stabilization

Integrin-mediated adhesion of cells to fibronectin induces microtubule stabilization (Palazzo et al., 2004), suggesting that ECM and paclitaxel might have additive effects on microtubules. The stabilizing effect of fibronectin requires integrin-mediated focal adhesion kinase (FAK) activation and Rho A (Palazzo et al., 2004). TGFBI is known to mediate adhesion also in an integrin-dependent manner (Billings et al., 2002; Nam et al., 2003; Jeong and Kim, 2004; Park et al., 2004). This suggested a model where TGFBI could modulate paclitaxel sensitivity via microtubule stabilizing effects (Figure 4A). rTGFBI promoted adhesion of SKOV-3 cells, and this effect was partially antagonized by pretreating cells with a blocking antibody to alphaV-beta3 integrin (Figures S5A and S5B) ($p < 0.001$, two-sided t test).

Figure 4B shows that cells plated on rTGFBI showed a significant increase in Glu-tubulin formation indicating microtubule stabilization (Gundersen et al., 1984; Palazzo et al., 2004). In addition, adhesion of cells to rTGFBI, or fibronectin, induced phosphorylation of FAK (Figure 4C). Attachment to fibronectin, but not to the integrin-independent adhesion peptide polylysine (PL), also showed Glu-tubulin formation (Figure 4D). To test whether FAK was required for microtubule stabilization by rTGFBI, we knocked down FAK in SKOV-3 cells using siRNAs, and these cells showed a significant decrease in microtubule stabilization following adhesion to rTGFBI (Figure 4E) ($p < 0.001$, two-sided t test). To test whether Rho A was

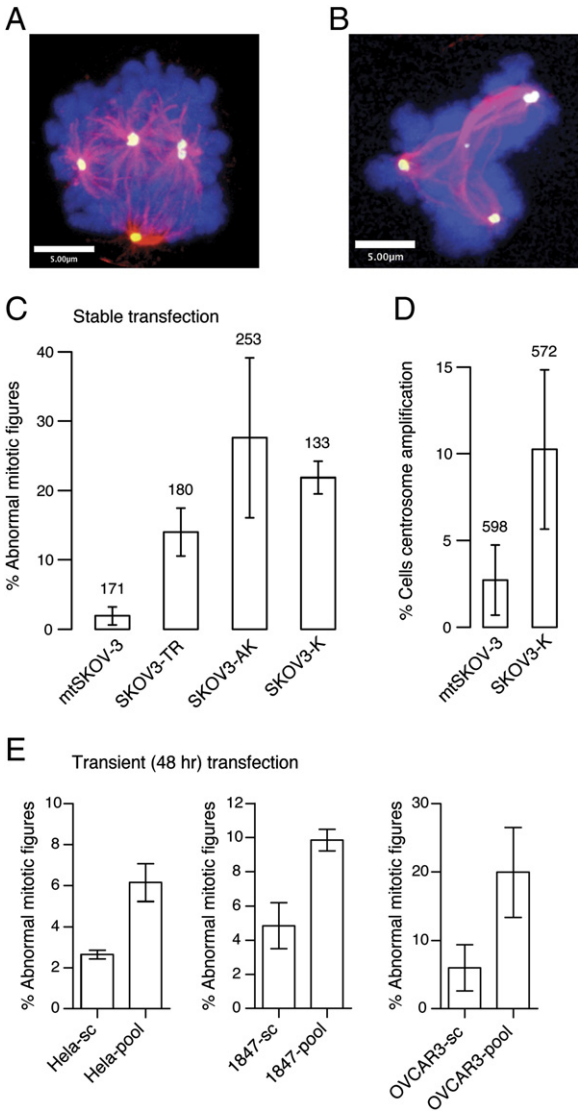

Figure 3. Loss of *TGFBI* Induces Mitotic Abnormalities

(A and B) Stable KD of *TGFBI* in SKOV-3 cells results in abnormal mitotic spindle formation and centrosome amplification. Magenta, tubulin; blue, Dapi-stained DNA; yellow, gamma tubulin.

(C) Proportion of abnormal mitotic cells at 9–30 days in SKOV-3TR, stable knockdown, and mock transfected (mt) cell line pools.

(D) Proportion of interphase cells showing centrosome amplification. Number of cells counted is shown above corresponding bars.

(E) Proportion of abnormal mitotic cells after 48 hr following transient knockdown of *TGFBI* using a pool of four siRNAs. Error bars show mean ± SD.

also required for rTGFBI microtubule stabilization, Rho A was specifically inactivated using the cell permeable inhibitor C3 toxin. This resulted in a significant decrease in microtubule stabilization following adhesion to rTGFBI (Figure 4F) ($p < 0.001$, two-sided t test). These data confirmed that rTGFBI induced microtubule stabilization and that this required intact FAK and Rho A signaling. Extension of these experiments to nonmalignant cells using NIH 3T3 fibroblasts also showed that rTGFBI induced Glu-tubulin formation and FAK phosphorylation (Figure S5C). In addition, inactivation of Rho in NIH 3T3 cells using a dominant-negative Rho A expression construct significantly reduced the rTGFBI-mediated stabilization of microtubules (Figure S5D).

rTGFBI Protein Sensitizes *TGFBI*-KD Cells to Paclitaxel in an Integrin-Dependent Manner

To test whether extracellular TGFBI was able to sensitize cells to the effect of paclitaxel, SKOV3-A and SKOV3-K cells were plated on rTGFBI-coated wells. This significantly increased paclitaxel-induced apoptosis ($p < 0.001$, two-way ANOVA) (Figure 5A). Importantly, KD of *TGFBI* significantly reduced the slope of the dose response curve for paclitaxel-induced Glu-tubulin formation (KD cells slope 1.3, 95% C. I. 0.6–2.1 versus SKOV-3 control cells slope 2.8, 95% C. I. 2.2–3.4) (Figures 5B and 5C). Plating KD cells on rTGFBI restored the slope of Glu-tubulin formation (slope 2.4, 95% C. I. 1.6–3.1) (Figures 5B and 5C and Figure S5E). SKOV-3TR cells plated on rTGFBI and treated with paclitaxel showed only a modest increase in apoptosis (data not shown), which we attributed to lower intracellular paclitaxel concentrations (Figure S2A). Increasing the level of intracellular paclitaxel by inhibiting paclitaxel efflux using verapamil significantly increased the sensitizing effect of rTGFBI in SKOV-3TR (Figure 5D). Verapamil also increased formation of stable microtubules in SKOV-3TR cells plated on rTGFBI following treatment with paclitaxel (Figure 5B). Control SKOV-3 cells plated on rTGFBI without paclitaxel treatment did not show increased caspase 3/7 activity (data not shown). We then tested whether rTGFBI was able to sensitize other paclitaxel-resistant ovarian cancer cells that had not been selected in vitro for resistance (see also Figure S1B). Figures 5E and 5F show that rTGFBI significantly increased paclitaxel-induced caspase activation in A2780 and PE0188 cells ($p < 0.001$, two-way ANOVA).

Incubation of *TGFBI*-KD cells in serum-free media conditioned with rTGFBI also resulted in a significant reversal of paclitaxel resistance ($p < 0.001$ one-way ANOVA) (Figure 5G and Figure S5F). To test whether this sensitization was integrin dependent, we pretreated SKOV3-K cells with anti-alphaVbeta3 blocking antibody before exposure to rTGFBI-conditioned media. This pretreatment significantly reduced paclitaxel-induced apoptosis ($p < 0.001$, one-way ANOVA), confirming that rTGFBI binding to alphaVbeta3 was required for paclitaxel sensitization (Figure 5G and Figure S5F). To examine whether microtubule stabilization was required for rTGFBI-mediated paclitaxel sensitization, we blocked Rho and FAK pathways downstream of rTGFBI-integrin binding. Pretreatment with C3 toxin of SKOV3-KD cells for 4 hr before paclitaxel treatment decreased the sensitizing effect of rTGFBI (Figure 5G and Figure S5F). Similarly, transient knockdown of FAK using a single siRNA blocked the sensitizing effect of rTGFBI in Figure 5G and Figure S5F.

FAK induces proliferation and survival in cancer cells, and therefore, downregulation of FAK was expected to

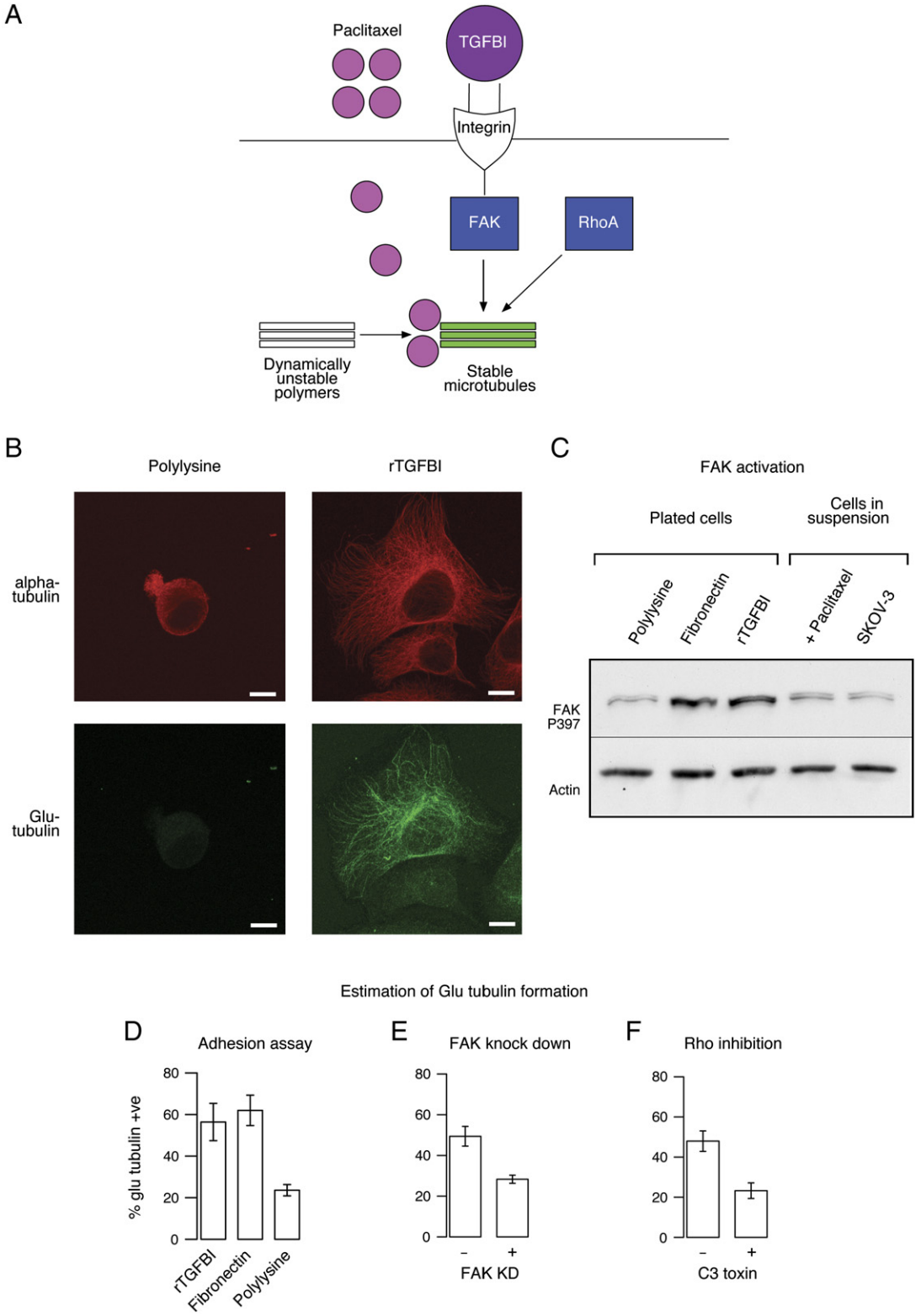

Figure 4. TGFBI Induces Microtubule Stabilization

(A) Model of TGFBI induction of microtubule stabilization.

(B) Microtubule stabilization demonstrated with anti-Glu tubulin antibody. SKOV-3 cells were plated for 90 min on rTGFBI or polylysine-coated glass slides (20 μg/ml) before immunofluorescence. Scale bars, 10 μm.

sensitize cells to chemotherapy (Judson et al., 1999; Sood et al., 2004). However, FAK is required for ECM-induced microtubule stabilization (Palazzo et al., 2004), and our data suggested that loss of FAK might also induce paclitaxel resistance. We have recently shown using a RNAi screen for all kinases (in which, therefore, *TGFBI* was not included) that loss of FAK (PTK2) and its family member PTK2B induced paclitaxel resistance in A549 non-small-cell lung carcinoma and HCT116 colon cancer cells, respectively (Swanton et al., 2007). Transient knockdown of FAK in SKOV-3 and breast cancer MDA-MB-231 cells (defined as paclitaxel sensitive, Figure S1B) using independent siRNAs also induced significant resistance to paclitaxel-mediated apoptosis ($p < 0.001$, two-way ANOVA) (Figure S5G and data not shown). In addition, inhibition of Rho A resulted in resistance to paclitaxel induced apoptosis (Figure S5H). These results show that perturbing components of pathways involved in microtubule stability is sufficient to induce paclitaxel resistance.

TGFBI Is Tightly Coexpressed with Fibronectin

In parallel with the in vitro work, we carried out a prospective randomized clinical trial (CTCR–OV01) specifically designed to examine the molecular response to carboplatin and paclitaxel monotherapy in patients with advanced ovarian cancer. Tumor samples were collected prior to the start of neoadjuvant therapy and at subsequent interval debulking surgery (Supplemental Data and Figure S6A).

As TGFBI is an integral component of the ECM, we investigated whether *TGFBI* expression correlated with the expression of other ECM transcripts that signal via integrins. We performed a correlation analysis between the expression of *TGFBI* and all other informative genes on the array ($n = 3426$), across all samples derived from patients treated with paclitaxel ($n = 20$), and ranked the genes according to their level of correlation with *TGFBI*. Strikingly, 18 out of the 20 top ranked genes were ECM-related genes (Table S2). Notably, these genes included fibronectin (*FN1*) ($r = 0.89$, Pearson correlation), collagen 5A1 (*COL5A1*) ($r = 0.83$, Pearson correlation), and thrombospondin-2 (*THBS2*) ($r = 0.88$, Pearson correlation). *THBS1* is a homolog of *THBS2* and was recently found to induce paclitaxel sensitivity through extracellular signaling (Lih et al., 2006). There was a significantly positive correlation between the probability of a gene being ECM-related and its degree of coexpression with *TGFBI* ($r = 0.89$, Pearson correlation; $p < 0.001$, linear regression) (Figure 6A).

To confirm this finding in external data sets, we analyzed published expression microarray data from ovarian and breast cancers (Spentzos et al., 2005; Naderi et al., 2007). Coregulation of *TGFBI* with ECM genes was reproduced with striking similarity (Figure 6B and data not shown). Importantly, the top ranked coexpressed genes in these independent sets consistently included fibronectin and *THBS2*. *THBS1* was also highly ranked in the Spentzos ovarian cancer data set (data not shown).

TGFBI Is Underexpressed in Paclitaxel-Resistant Primary Ovarian Carcinoma Tissues

To determine whether *TGFBI* expression was associated with clinical paclitaxel resistance, we analyzed microarray expression data from twenty patients randomized to paclitaxel monotherapy in CTCR-OV01. Patients who showed paclitaxel resistance, as indicated by CA125 monitoring, had a significantly lower expression of *TGFBI* ($p = 0.046$, Wilcoxon test; 3.9% false discovery rate). RNA from 16/20 samples was available for real-time PCR. Patients who showed no paclitaxel response had a significantly lower expression of *TGFBI* ($p = 0.0087$, $n = 16$, Wilcoxon test) in their pretreatment samples compared to those who responded (Figure 6C).

Centrosome Amplification Is Present in Paclitaxel-Resistant Ovarian Cancer Samples

As loss of *TGFBI* resulted in spindle deformities and centrosome amplification, we examined whether centrosome amplification correlated with paclitaxel resistance in clinical samples. To accurately count centrosomes in samples from the clinical study, we used three-dimensional reconstructions of confocal images from 20 μm tissue sections. Adequate amounts of tumor tissue were available in 10 pretreatment samples. Reconstructed images were scored by rotating the image to count the number of centrosomes associated with each nucleus (Figure 6D and Movie S1). Using this method, a total number of 2376 nuclei were examined in 10 cancer samples, and counting was performed blind to the clinical outcome of patients. We found a significantly higher ($p = 0.019$, Wilcoxon test) proportion of cells with centrosome amplification in paclitaxel-resistant patients (7.6%) compared to paclitaxel responders (3.9%) (Figure 6E).

Paclitaxel-Induced Cell Death in Ovarian Cancer Samples Colocalizes with Areas of High TGFBI Protein Expression

We next examined ovarian cancer samples taken after paclitaxel treatment from the CTCR-OV01 study using immunohistochemistry for TGFBI. Sections of ovarian cancer tissue revealed morphological changes typical of paclitaxel-induced cytotoxicity, including cytoplasmic vacuolation and multinucleation (Seiler et al., 2004), and

(C) Cells were adhered to polylysine, fibronectin, or rTGFBI-coated wells (20 μg/ml) for 90 min before lysates were collected for immunoblotting using anti-phosphorylated FAK (P397). Also shown are immunoblots for lysates of cells treated in suspension with or without paclitaxel at 3 μM.
(D) Percentages of SKOV-3 cells showing Glu-tubulin following adhesion to rTGFBI, fibronectin, or polylysine.
(E) 48 hr following transfection using either FAK siRNA or nontargeting siRNAs, SKOV-3 cells were plated on rTGFBI coated glass slides for 90 min and the percentage of cells showing Glu-tubulin formation was estimated by immunofluorescence.
(F) SKOV-3 cells were either treated with the Rho A inhibitor C3 toxin in SFM or with SFM alone for 4 hr before plating on rTGFBI-coated glass slides and estimation of Glu-tubulin formation. Error bars show mean ± SD.

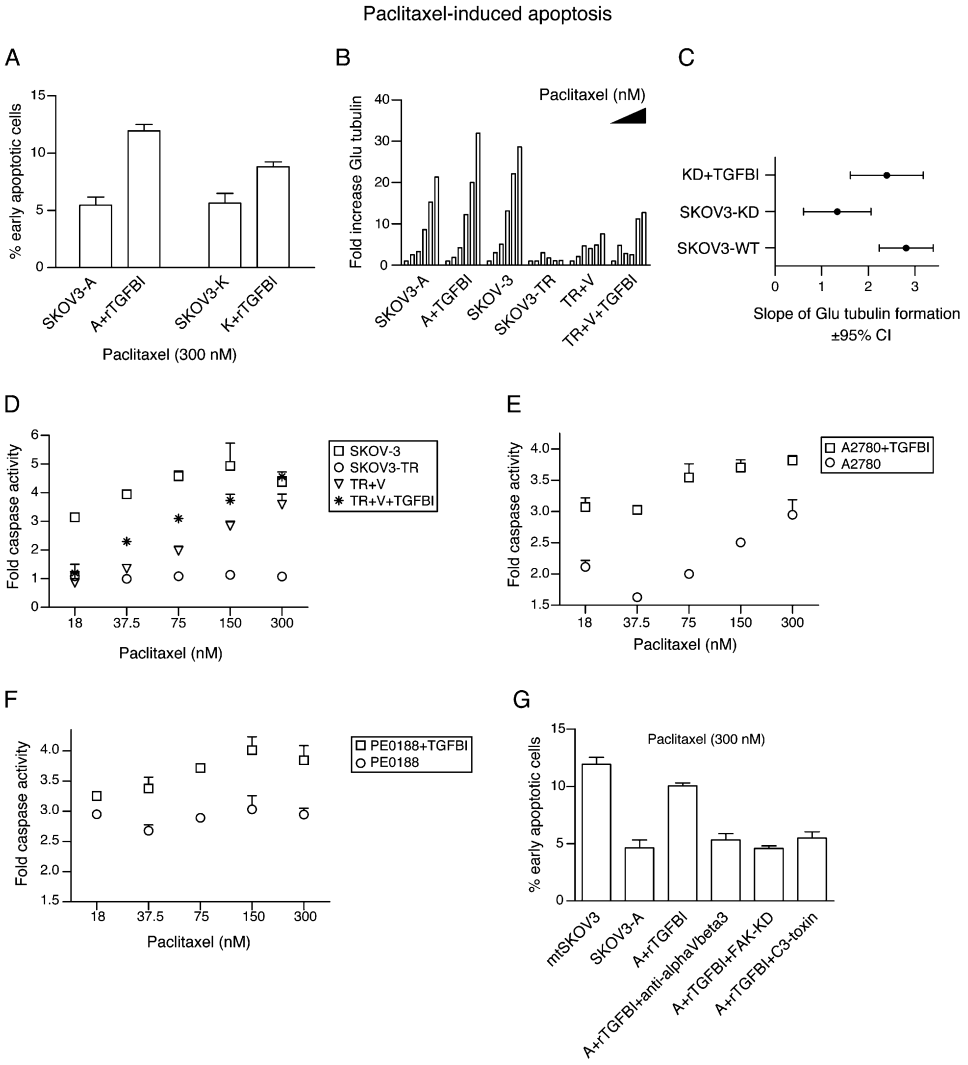

Figure 5. rTGFBI Sensitizes Resistant Cells to the Effect of Paclitaxel

(A) Cells were adhered to rTGFBI-coated wells (20 μg/ml) or noncoated wells for 24 hr prior to paclitaxel treatment for 48 hr. Shown is the percentage of apoptotic cells as measured using FITC-annexin V and 7-AAD staining.

(B) Cells were serum starved for 24 hr then treated with paclitaxel in serum-free medium (SFM) at 0, 4, 16, 75, 300, and 1200 nM concentrations for 1 hour before lysates were collected for fluorescence immunoblotting using anti-Glu-tubulin and anti-alpha tubulin. Bars represent the fold increase in glu-tubulin fluorescence intensity values normalized for alpha tubulin intensity values. Filled triangle indicates increasing paclitaxel dose across each group of bars.

(C) The slope and 95% confidence intervals for the linear regression of Glu-tubulin formation following paclitaxel treatment in SKOV-3 and mtSKOV3 (SKOV3-WT), SKOV3-A and SKOV3-K (SKOV3-KD), and SKOV3-KD following plating on rTGFBI.

(D) SKOV-3TR cells were either plated on plastic or rTGFBI as in (A) and either treated with paclitaxel alone (SKOV3-TR) or with paclitaxel and verapamil 3.3 μM (TR + V and TR + V + rTGFBI) for 48 hr before caspase 3/7 activity was estimated. Also shown is the data for the parental sensitive line (SKOV-3) plated on plastic.

(E and F) A2780 Cells (E) or PE0188 cells (F) were either plated on plastic or on rTGFBI (20 μg/ml) before paclitaxel treatment for 48 hr. Shown is the fold increase in caspase 3/7 activity.

(G) Cells were either pretreated with 50 μg/ml of rTGFBI in SFM or SFM alone for 2 hr followed by paclitaxel treatment for 1 hr, washing, and incubation in full media for 48 hr. Shown is the percentage of apoptotic cells measured by FITC-annexin V and 7-AAD staining. A+rTGFBI+anti-alphaVbeta3; SKOV3-A cells pretreated with anti-alphaVbeta3 in SFM before treatment with rTGFBI and paclitaxel, A+rTGFBI+FAK-KD; SKOV3-A cells were transfected with siRNA targeting FAK 48 hr prior to rTGFBI and paclitaxel treatment, A+rTGFBI+C3-toxin; SKOV3-A cells were pretreated with the Rho A inhibitor, C3 toxin, in SFM for 4 hr before the application of rTGFBI and paclitaxel. Error bars show mean ± SD.

these changes were localized to areas of high TGFBI staining (Figure 6F and Figures S6B and S6C). TGFBI labeling was absent in the ECM around neighboring cells lacking paclitaxel-induced changes and in areas of necrosis (Figure 6F and Figure S6D). Positive TGFBI staining was significantly associated with evidence of paclitaxel-induced

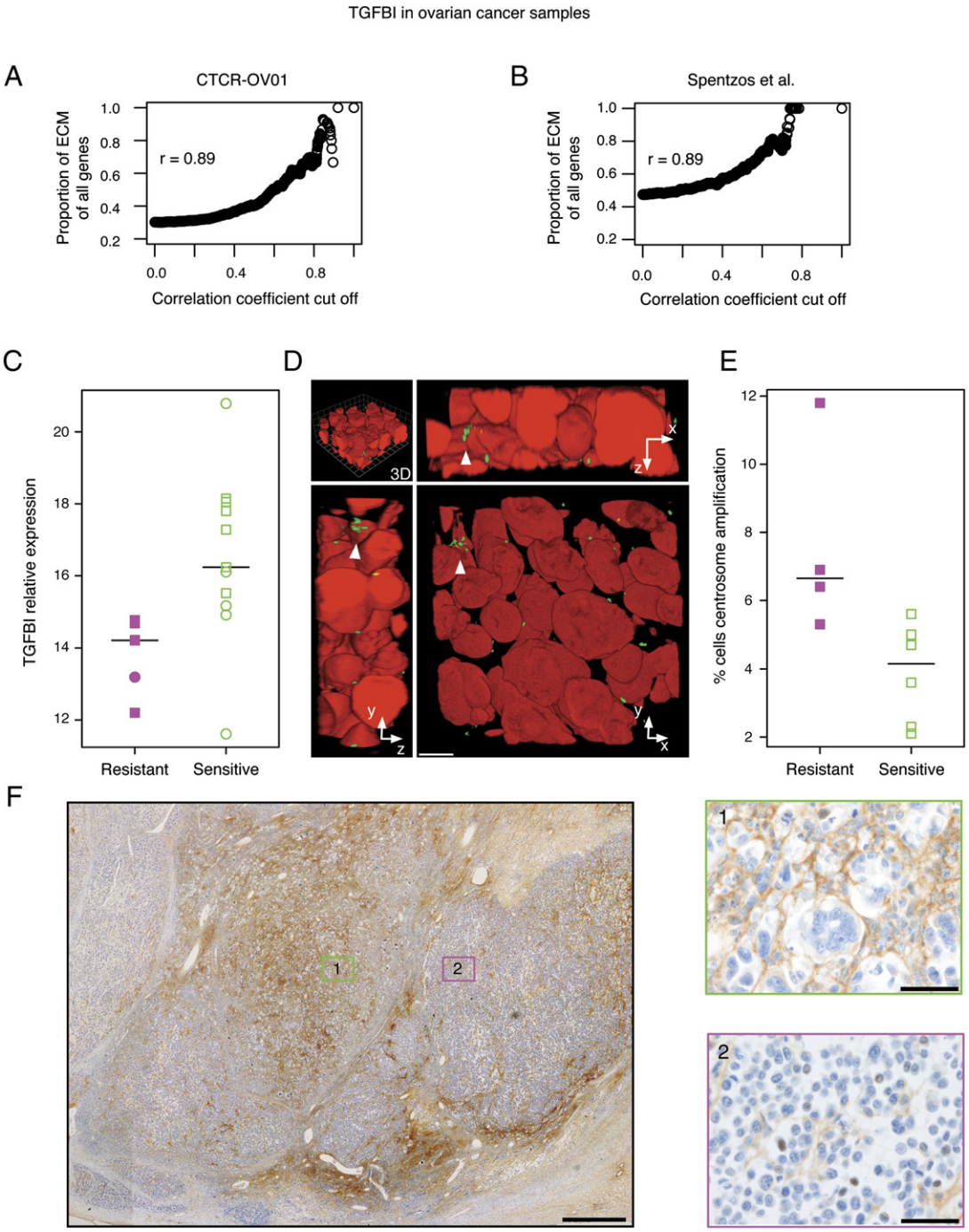

Figure 6. The ECM Protein TGFBI Sensitizes Ovarian Carcinoma Cells In Vivo to the Effect of Paclitaxel

Correlation between expression of *TGFBI* and ECM genes in (A) CTCR-OV01 study and (B) independent ovarian cancer data set from Spentzos et al. (2005). Graphs show proportion of ECM-related genes increasing as a function of coexpression with *TGFBI*. (C) *TGFBI* expression in pretreatment biopsies of advanced ovarian carcinoma using real-time PCR. Resistant cases (n = 5; magenta) are compared to sensitive cases (n = 11; green). (D) Three-dimensional reconstruction of Z stack images obtained following double immunofluorescent staining of a representative ovarian carcinoma tissue section. Arrowheads indicate amplified centrosomes in a single cell confirmed by examination in all three planes. Anti-γ tubulin, green; chromosomal DNA, Hoechst 33258 red. Scale bar, 10 μm. (E) Centrosome amplification is associated with paclitaxel resistance. Centrosome counting was performed on samples from which adequate frozen tissue was available (n = 10; samples common between [C] and [E] are indicated by squares). In (C) and (E), horizontal bars indicate median values. (F) Immunohistochemistry for TGFBI of representative posttreatment ovarian cancer sample. Paclitaxel-induced morphological changes colocalize with focal TGFBI expression (brown staining, green box 1) but not in areas of low TGFBI expression (magenta box 2). Scale bars for main subfigure and boxes, 500 μm and 50 μm, respectively.

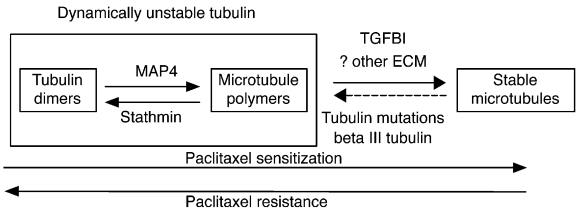

Figure 7. Proposed Model of Modulation of Paclitaxel Resistance by TGFBI via Effects on Microtubule Stability

cytotoxicity (n = 14, p = 0.0035, Chi square test with Monte-Carlo simulation). Importantly, focal TGFBI staining was present in pretreatment samples; however cytoplasmic vacuolation and multinucleation were not seen (Figure S6E).

DISCUSSION

Our results suggest that the ECM protein TGFBI modulates paclitaxel response via regulation of microtubule stability. Acetylated and detyrosinated microtubules define a stable subpopulation of microtubule polymers that resist depolymerization (Gundersen et al., 1984). This population is less dynamic compared to unstable microtubules and, therefore, less likely to contribute to the proportion of depolymerized tubulin in the cell (Figure 7). As paclitaxel primarily targets polymerized microtubules, an increase in the proportion of unstable microtubules induces paclitaxel resistance (Gonçalves et al., 2001; Barlow et al., 2002; Hari et al., 2006). We show that extracellular TGFBI stabilized microtubules and increased sensitivity to paclitaxel. Conversely, selective loss of *TGFBI* by KD resulted in mitotic spindle abnormalities and paclitaxel resistance. These findings mimic previous results from cell lines with intracellular alterations of tubulin that also caused paclitaxel resistance and mitotic instability (Gonçalves et al., 2001; Martello et al., 2003). TGFBI was originally identified as induced by TGFβ stimulation in adenocarcinoma cells (Skonier et al., 1992), and our results may explain how TGFβ induces microtubule stabilization in serum-starved fibroblasts (Gundersen et al., 1994). Recombinant TGFBI induced microtubule stabilization that was dependent on integrin-mediated FAK and Rho signaling. The exact mechanisms of microtubule stabilization downstream of FAK and Rho remain unknown but may include mDIA1 or inactivation of the microtubule associated protein stathmin (Palazzo et al., 2004; Baldassarre et al., 2005).

The relationship between ECM proteins and drug resistance is likely to be complex. Previous studies have shown that ECM proteins induced resistance to DNA-damaging drugs such as cisplatin and etoposide, and decreased apoptosis was associated with β1-integrin-mediated activation of PI3K and AKT (Sethi et al., 1999; Hodkinson et al., 2006). In contrast, the ECM protein THBS1 sensitizes pancreatic cancer cells specifically to taxane-induced apoptosis in a CD47-dependent manner (Lih et al., 2006). Here, we show that *TGFBI* is tightly coexpressed with THBS1 in ovarian and breast cancers. It is possible that the two proteins may cooperate to induce taxane sensitization through activating CD47-driven pathways (THBS1) and integrin-mediated microtubule stabilization (TGFBI). The finding that the protein expression of TGFBI in tissue samples treated with paclitaxel monotherapy, specifically colocalized with areas of taxane-induced cytotoxicity suggests that TGFBI, and possibly other ECM proteins, modulate taxane effects in vivo. Our data extend previous reports and suggests that the specific molecular targets of individual drugs are likely to determine whether the effect of the ECM is agonistic or antagonistic with chemotherapy.

Importantly the findings reported here have potentially significant clinical implications. First, TGFBI protein expression is lost in a third of primary ovarian cancers (A.A.A., A.E.K.I., and J.D.B., unpublished data) and *TGFBI* has previously been shown to be methylated and downregulated in lung cancer (Shao et al., 2006; Zhao et al., 2006). Future studies should correlate the expression of TGFBI with taxane response to test the value of TGFBI as a predictive biomarker. Second, in ovarian cancer, FAK is overexpressed, plays a role in regulating invasion and metastasis, and is associated with poor clinical outcome (Judson et al., 1999; Sood et al., 2004). FAK also regulates tumor growth either directly, through activation of ERK-dependent pathways (Hecker et al., 2002), or indirectly through inducing angiogenesis (Sheta et al., 2000). Downregulation of FAK using siRNAs results in inhibited growth and metastasis of pancreatic cancer (Duxbury et al., 2004) and could, therefore, be attractive therapeutically. However, previous studies have demonstrated that FAK is required for adhesion-dependent microtubule stabilization (Palazzo et al., 2004). In the current study, loss of FAK or Rho A blocked microtubule stabilization and paclitaxel sensitization by rTGFBI. Importantly, and in contrast to previous publications (Halder et al., 2005), our results show that loss of FAK results in increased resistance to taxanes, and this was confirmed using independent siRNAs and experimental studies (Swanton et al., 2007). As FAK is low or absent in one-third of patients with ovarian cancer (Sood et al., 2004), it could be used as a marker to identify patients who may not benefit from paclitaxel treatment. Furthermore, although downregulation of FAK may also induce growth inhibition, our data argue against combining FAK inhibitors with paclitaxel treatment.

We describe here a mechanism of specific paclitaxel sensitization via induction of microtubule stabilization by the ECM protein TGFBI. Furthermore, we show that expression of *TGFBI* in ovarian and breast tumors is tightly coregulated with other ECM proteins that either induce microtubule stabilization or paclitaxel sensitization. The effectiveness of taxanes in improving survival in ovarian cancer remains controversial (International Collaborative Ovarian Neoplasm Group, 2002), and TGFBI could be used as a biomarker for selecting patients for taxane therapy. In addition, as TGFBI is an ECM protein, activating peptides or antibodies that mimic its action may be a strategy for modulation of response to taxane chemotherapy.

EXPERIMENTAL PROCEDURES

Cambridge Translational Cancer Research Ovary 01 Study

The details of this study are described in Supplemental Experimental Procedures. The study was approved by the Cambridge Local Research Ethics Committee (LREC). All patients gave written informed consent prior to participation.

Cell Culture

Cell lines were obtained from Cell Services (Cancer Research UK London Research Institute) and were maintained in RPMI 140 medium supplemented with 10% fetal bovine serum, penicillin, and streptomycin and incubated at 37°C and 5% CO2. SKOV-3TR cells were maintained in 0.3 μM paclitaxel.

Apoptosis Assays, Annexin V Binding, and Flow Cytometric Analyses

Cells were grown in 6-well plates to 80% confluence before paclitaxel, nocodazole, cisplatin, or verapamil treatment (Sigma). For rTGFBI pretreatment experiments, adherent cells in 24-well tissue culture plates were incubated with rTGFBI at 50 μg/ml in serum-free media (SFM) for 2 hr followed by paclitaxel treatment for 1 hr to make up the required concentrations. Cells were then washed with PBS and incubated with normal media for 48 hr. For integrin-blocking experiments, attached cells were incubated with the mouse monoclonal antibody anti-alphaVbeta3 (Chemicon) for 1 hr (1 in 100 dilution) in SFM. Rho A inhibition in SKOV-3 cells was achieved by treating attached cells with 2 μg/ml cell permeable C3 transferase recombinant protein (Cytoskeleton) in SFM for 4 hr prior to paclitaxel treatment for 1 hr. Early apoptosis was estimated using apoptosis detection kit (R & D systems) and 7-AAD (Molecular Probes) following the manufacturers' instructions and as previously described (Wang et al., 1998). Flow cytometric analysis was performed with a LSR II flow cytometer (BD bioscience) and analyzed with the FACSDiva software (BD bioscience).

Caspase 3 and 7 Assays

We first confirmed the optimum number of cells and linear range for paclitaxel dose response for the assay. Cells were plated at 1×10^4 cells per well in a 384-well plate in 20 μl volume overnight before paclitaxel was added in 10 μl volume to reach the final indicated concentrations. Caspase 3/7 activity was estimated 48 hr following treatment by adding 30 μl of the Caspase-Glo 3/7 Assay reagent (Promega). Luminescence was read following at least 1 hr of incubation on a luminescence plate reader (Infinite M200, Tecan) using the i-control software (Tecan).

Supplemental Data

The Supplemental Data include Supplemental Experimental Procedures, five supplemental figures, two supplemental tables, and one supplemental movie and can be found with this article online at http://www.cancercell.org/cgi/content/full/12/6/514/DC1/.

ACKNOWLEDGMENTS

This work was supported by Cancer Research UK (CR-UK) and the Medical Research Council (MRC). A.A.A. and C.S. hold CR-UK Clinician Scientist Fellowships. C.B. was funded by the National Translational Cancer Research Network (NTRAC). N.G.I. was a recipient of a National Medical Research Council (Singapore) Medical Research Fellowship. We thank our patients and members of the Gynaecological Oncology Multidisciplinary Team at Cambridge University Hospitals NHS Foundation Trust for their participation in the CTCR-OV01 clinical study. We thank Drs. Shin-Ichi Ohnuma, Daniel F. Schorderet, and Ching Yuan for gifts of reagents; Dr. Andrew E. Teschendorff for sharing unpublished data; and Lysa Baginsky and John Brown for expert technical assistance. We are also grateful to Drs. Fanni Gergely, Masashi Narita, and Natalie Thorne for helpful discussions.

Received: March 23, 2007
Revised: August 17, 2007
Accepted: November 19, 2007
Published: December 10, 2007

REFERENCES

Alli, E., Bash-Babula, J., Yang, J.M., and Hait, W.N. (2002). Effect of stathmin on the sensitivity to antimicrotubule drugs in human breast cancer. Cancer Res. *62*, 6864–6869.

Anand, S., Penrhyn-Lowe, S., and Venkitaraman, A.R. (2003). AURORA-A amplification overrides the mitotic spindle assembly checkpoint, inducing resistance to Taxol. Cancer Cell *3*, 51–62.

Baldassarre, G., Belletti, B., Nicoloso, M.S., Schiappacassi, M., Vecchione, A., Spessotto, P., Morrione, A., Canzonieri, V., and Colombatti, A. (2005). p27(Kip1)-stathmin interaction influences sarcoma cell migration and invasion. Cancer Cell *7*, 51–63.

Barlow, S.B., Gonzalez-Garay, M.L., and Cabral, F. (2002). Paclitaxel-dependent mutants have severely reduced microtubule assembly and reduced tubulin synthesis. J. Cell Sci. *115*, 3469–3478.

Billings, P.C., Whitbeck, J.C., Adams, C.S., Abrams, W.R., Cohen, A.J., Engelsberg, B.N., Howard, P.S., and Rosenbloom, J. (2002). The transforming growth factor-beta-inducible matrix protein (beta)ig-h3 interacts with fibronectin. J. Biol. Chem. *277*, 28003–28009.

Cook, T.A., Nagasaki, T., and Gundersen, G.G. (1998). Rho guanosine triphosphatase mediates the selective stabilization of microtubules induced by lysophosphatidic acid. J. Cell Biol. *141*, 175–185.

Duan, Z., Feller, A.J., Toh, H.C., Makastorsis, T., and Seiden, M.V. (1999). TRAG-3, a novel gene, isolated from a taxol-resistant ovarian carcinoma cell line. Gene *229*, 75–81.

Duan, Z., Lamendola, D.E., Duan, Y., Yusuf, R.Z., and Seiden, M.V. (2005). Description of paclitaxel resistance-associated genes in ovarian and breast cancer cell lines. Cancer Chemother. Pharmacol. *55*, 277–285.

Duxbury, M.S., Ito, H., Zinner, M.J., Ashley, S.W., and Whang, E.E. (2004). Focal adhesion kinase gene silencing promotes anoikis and suppresses metastasis of human pancreatic adenocarcinoma cells. Surgery *135*, 555–562.

Giannakakou, P., Sackett, D.L., Kang, Y.K., Zhan, Z., Buters, J.T., Fojo, T., and Poruchynsky, M.S. (1997). Paclitaxel-resistant human ovarian cancer cells have mutant beta-tubulins that exhibit impaired paclitaxel-driven polymerization. J. Biol. Chem. *272*, 17118–17125.

Gonçalves, A., Braguer, D., Kamath, K., Martello, L., Briand, C., Horwitz, S., Wilson, L., and Jordan, M.A. (2001). Resistance to Taxol in lung cancer cells associated with increased microtubule dynamics. Proc. Natl. Acad. Sci. USA *98*, 11737–11742.

Gundersen, G.G., Kalnoski, M.H., and Bulinski, J.C. (1984). Distinct populations of microtubules: Tyrosinated and nontyrosinated alpha tubulin are distributed differently in vivo. Cell *38*, 779–789.

Gundersen, G.G., Kim, I., and Chapin, C.J. (1994). Induction of stable microtubules in 3T3 fibroblasts by TGF-beta and serum. J. Cell Sci. *107*, 645–659.

Halder, J., Landen, C.N., Jr., Lutgendorf, S.K., Li, Y., Jennings, N.B., Fan, D., Nelkin, G.M., Schmandt, R., Schaller, M.D., and Sood, A.K. (2005). Focal adhesion kinase silencing augments docetaxel-mediated apoptosis in ovarian cancer cells. Clin. Cancer Res. *11*, 8829–8836.

Hari, M., Loganzo, F., Annable, T., Tan, X., Musto, S., Morilla, D.B., Nettles, J.H., Snyder, J.P., and Greenberger, L.M. (2006). Paclitaxel-resistant cells have a mutation in the paclitaxel-binding region of beta-tubulin (Asp26Glu) and less stable microtubules. Mol. Cancer Ther. *5*, 270–278.

Hecker, T.P., Grammer, J.R., Gillespie, G.Y., Stewart, G., and Gladson, C.L. (2002). Focal adhesion kinase enhances signaling through the Shc/extracellular signal-regulated kinase pathway in anaplastic astrocytoma tumor biopsy samples. Cancer Res. *62*, 2699–2707.

Hodkinson, P.S., Elliott, T., Wong, W.S., Rintoul, R.C., Mackinnon, A.C., Haslett, C., and Sethi, T. (2006). ECM overrides DNA damage-induced cell cycle arrest and apoptosis in small-cell lung cancer cells through beta1 integrin-dependent activation of PI3-kinase. Cell Death Differ. *13*, 1776–1788.

Huang, J.C., Zamble, D.B., Reardon, J.T., Lippard, S.J., and Sancar, A. (1994). HMG-domain proteins specifically inhibit the repair of the major DNA adduct of the anticancer drug cisplatin by human excision nuclease. Proc. Natl. Acad. Sci. USA *91*, 10394–10398.

Huang, Y., Ray, S., Reed, J.C., Ibrado, A.M., Tang, C., Nawabi, A., and Bhalla, K. (1997). Estrogen increases intracellular p26Bcl-2 to p21Bax ratios and inhibits taxol-induced apoptosis of human breast cancer MCF-7 cells. Breast Cancer Res. Treat. *42*, 73–81.

Ibrado, A.M., Kim, C.N., and Bhalla, K. (1998). Temporal relationship of CDK1 activation and mitotic arrest to zytosolic accumulation of cytochrome C and caspase-3 activity during Taxol-induced apoptosis of human AML HL-60 cells. Leukemia *12*, 1930–1936.

International Collaborative Ovarian Neoplasm Group (2002). Paclitaxel plus carboplatin versus standard chemotherapy with either single-agent carboplatin or cyclophosphamide, doxorubicin, and cisplatin in women with ovarian cancer: The ICON3 randomised trial. Lancet *360*, 505–515.

Jeong, H.W., and Kim, I.S. (2004). TGF-beta1 enhances betaig-h3-mediated keratinocyte cell migration through the alpha3beta1 integrin and PI3K. J. Cell. Biochem. *92*, 770–780.

Judson, P.L., He, X., Cance, W.G., and Van Le, L. (1999). Overexpression of focal adhesion kinase, a protein tyrosine kinase, in ovarian carcinoma. Cancer *86*, 1551–1556.

Kasparkova, J., Delalande, O., Stros, M., Elizondo-Riojas, M.A., Vojtiskova, M., Kozelka, J., and Brabec, V. (2003). Recognition of DNA interstrand cross-link of antitumor cisplatin by HMGB1 protein. Biochemistry *42*, 1234–1244.

Kline-Smith, S.L., and Walczak, C.E. (2004). Mitotic spindle assembly and chromosome segregation: Refocusing on microtubule dynamics. Mol. Cell *15*, 317–327.

Lamendola, D.E., Duan, Z., Yusuf, R.Z., and Seiden, M.V. (2003). Molecular description of evolving paclitaxel resistance in the SKOV-3 human ovarian carcinoma cell line. Cancer Res. *63*, 2200–2205.

Lih, C.J., Wei, W., and Cohen, S.N. (2006). Txr1: A transcriptional regulator of thrombospondin-1 that modulates cellular sensitivity to taxanes. Genes Dev. *20*, 2082–2095.

Logarinho, E., Bousbaa, H., Dias, J.M., Lopes, C., Amorim, I., Antunes-Martins, A., and Sunkel, C.E. (2004). Different spindle checkpoint proteins monitor microtubule attachment and tension at kinetochores in Drosophila cells. J. Cell Sci. *117*, 1757–1771.

Martello, L.A., Verdier-Pinard, P., Shen, H.J., He, L., Torres, K., Orr, G.A., and Horwitz, S.B. (2003). Elevated levels of microtubule destabilizing factors in a Taxol-resistant/dependent A549 cell line with an alpha-tubulin mutation. Cancer Res. *63*, 1207–1213.

McGuire, W.P., Hoskins, W.J., Brady, M.F., Kucera, P.R., Partridge, E.E., Look, K.Y., Clarke-Pearson, D.L., and Davidson, M. (1996). Cyclophosphamide and cisplatin compared with paclitaxel and cisplatin in patients with stage III/IV ovarian cancer). N. Engl. J. Med. *334*, 1–6.

Mozzetti, S., Ferlini, C., Concolino, P., Filippetti, F., Raspaglio, G., Prislei, S., Gallo, D., Martinelli, E., Ranelletti, F.O., Ferrandina, G., et al. (2005). Class III beta-tubulin overexpression is a prominent mechanism of paclitaxel resistance in ovarian cancer patients. Clin. Cancer Res. *11*, 298–305.

Naderi, A., Teschendorff, A.E., Barbosa-Morais, N.L., Pinder, S.E., Green, A.R., Powe, D.G., Robertson, J.F., Aparicio, S., Ellis, I.O., Brenton, J.D., et al. (2007). A gene-expression signature to predict survival in breast cancer across independent data sets. Oncogene *26*, 1507–1516.

Nam, J.O., Kim, J.E., Jeong, H.W., Lee, S.J., Lee, B.H., Choi, J.Y., Park, R.W., Park, J.Y., and Kim, I.S. (2003). Identification of the alphavbeta3 integrin-interacting motif of betaig-h3 and its anti-angiogenic effect. J. Biol. Chem. *278*, 25902–25909.

Nicklas, R.B. (1997). How cells get the right chromosomes. Science *275*, 632–637.

Palazzo, A.F., Eng, C.H., Schlaepfer, D.D., Marcantonio, E.E., and Gundersen, G.G. (2004). Localized stabilization of microtubules by integrin- and FAK-facilitated Rho signaling. Science *303*, 836–839.

Park, S.W., Bae, J.S., Kim, K.S., Park, S.H., Lee, B.H., Choi, J.Y., Park, J.Y., Ha, S.W., Kim, Y.L., Kwon, T.H., et al. (2004). Beta ig-h3 promotes renal proximal tubular epithelial cell adhesion, migration and proliferation through the interaction with alpha3beta1 integrin. Exp. Mol. Med. *36*, 211–219.

Peer, D., Dekel, Y., Melikhov, D., and Margalit, R. (2004). Fluoxetine inhibits multidrug resistance extrusion pumps and enhances responses to chemotherapy in syngeneic and in human xenograft mouse tumor models. Cancer Res. *64*, 7562–7569.

Sandler, A., Gray, R., Perry, M.C., Brahmer, J., Schiller, J.H., Dowlati, A., Lilenbaum, R., and Johnson, D.H. (2006). Paclitaxel-carboplatin alone or with bevacizumab for non-small-cell lung cancer. N. Engl. J. Med. *355*, 2542–2550.

Scatena, C.D., Stewart, Z.A., Mays, D., Tang, L.J., Keefer, C.J., Leach, S.D., and Pietenpol, J.A. (1998). Mitotic phosphorylation of Bcl-2 during normal cell cycle progression and Taxol-induced growth arrest. J. Biol. Chem. *273*, 30777–30784.

Schiff, P.B., Fant, J., and Horwitz, S.B. (1979). Promotion of microtubule assembly in vitro by taxol. Nature *277*, 665–667.

Schiff, P.B., and Horwitz, S.B. (1980). Taxol stabilizes microtubules in mouse fibroblast cells. Proc. Natl. Acad. Sci. USA *77*, 1561–1565.

Seiler, N., Schneider, Y., Gossé, F., Schleiffer, R., and Raul, F. (2004). Polyploidisation of metastatic colon carcinoma cells by microtubule and tubulin interacting drugs: Effect on proteolytic activity and invasiveness. Int. J. Oncol. *25*, 1039–1048.

Sethi, T., Rintoul, R.C., Moore, S.M., MacKinnon, A.C., Salter, D., Choo, C., Chilvers, E.R., Dransfield, I., Donnelly, S.C., Strieter, R., et al. (1999). Extracellular matrix proteins protect small cell lung cancer cells against apoptosis: A mechanism for small cell lung cancer growth and drug resistance in vivo. Nat. Med. *5*, 662–668.

Shao, G., Berenguer, J., Borczuk, A.C., Powell, C.A., Hei, T.K., and Zhao, Y. (2006). Epigenetic inactivation of Betaig-h3 gene in human cancer cells. Cancer Res. *66*, 4566–4573.

Sheta, E.A., Harding, M.A., Conaway, M.R., and Theodorescu, D. (2000). Focal adhesion kinase, Rap1, and transcriptional induction of vascular endothelial growth factor. J. Natl. Cancer Inst. *92*, 1065–1073.

Skonier, J., Neubauer, M., Madisen, L., Bennett, K., Plowman, G.D., and Purchio, A.F. (1992). cDNA cloning and sequence analysis of beta ig-h3, a novel gene induced in a human adenocarcinoma cell line after treatment with transforming growth factor-beta. DNA Cell Biol. *11*, 511–522.

Sood, A.K., Coffin, J.E., Schneider, G.B., Fletcher, M.S., DeYoung, B.R., Gruman, L.M., Gershenson, D.M., Schaller, M.D., and Hendrix, M.J. (2004). Biological significance of focal adhesion kinase in ovarian cancer: Role in migration and invasion. Am. J. Pathol. *165*, 1087–1095.

Spentzos, D., Levine, D.A., Kolia, S., Otu, H., Boyd, J., Libermann, T.A., and Cannistra, S.A. (2005). Unique gene expression profile based on pathologic response in epithelial ovarian cancer. J. Clin. Oncol. *23*, 7911–7918.

Swanton, C., Marani, M., Pardo, O., Warne, P.H., Kelly, G., Sahai, E., Elustondo, F., Chang, J., Temple, J., Ahmed, A.A., et al. (2007). Regulators of mitotic arrest and ceramide metabolism are determinants of sensitivity to paclitaxel and other chemotherapeutic drugs. Cancer Cell *11*, 1–15.

Tan, M., Jing, T., Lan, K.H., Neal, C.L., Li, P., Lee, S., Fang, D., Nagata, Y., Liu, J., Arlinghaus, R., et al. (2002). Phosphorylation on tyrosine-15

of p34(Cdc2) by ErbB2 inhibits p34(Cdc2) activation and is involved in resistance to taxol-induced apoptosis. Mol. Cell *9*, 993–1004.

Taxman, D.J., MacKeigan, J.P., Clements, C., Bergstralh, D.T., and Ting, J.P. (2003). Transcriptional profiling of targets for combination therapy of lung carcinoma with paclitaxel and mitogen-activated protein/extracellular signal-regulated kinase kinase inhibitor. Cancer Res. *63*, 5095–5104.

Ueta, E., Yoneda, K., Kimura, T., Tatemoto, Y., Doi, S., Yamamoto, T., and Osaki, T. (2001). Mn-SOD antisense upregulates in vivo apoptosis of squamous cell carcinoma cells by anticancer drugs and gamma-rays regulating expression of the BCL-2 family proteins, COX-2 and p21. Int. J. Cancer *94*, 545–550.

Wang, T.H., Wang, H.S., Ichijo, H., Giannakakou, P., Foster, J.S., Fojo, T., and Wimalasena, J. (1998). Microtubule-interfering agents activate c-Jun N-terminal kinase/stress-activated protein kinase through both Ras and apoptosis signal-regulating kinase pathways. J. Biol. Chem. *273*, 4928–4936.

Wang, Y., Veeraraghavan, S., and Cabral, F. (2004). Intra-allelic suppression of a mutation that stabilizes microtubules and confers resistance to colcemid. Biochemistry *43*, 8965–8973.

Zhang, C.C., Yang, J.M., White, E., Murphy, M., Levine, A., and Hait, W.N. (1998). The role of MAP4 expression in the sensitivity to paclitaxel and resistance to vinca alkaloids in p53 mutant cells. Oncogene *16*, 1617–1624.

Zhao, Y., El-Gabry, M., and Hei, T.K. (2006). Loss of Betaig-h3 protein is frequent in primary lung carcinoma and related to tumorigenic phenotype in lung cancer cells. Mol. Carcinog. *45*, 84–92.

Accession Numbers

The microarray data tables are available from the Gene Expression Omnibus (GEO) at http://www.ncbi.nlm.nih.gov/geo/. Series numbers, GSE2627 and GSE9455 for cell lines and CTCR-OV01 study, respectively.